Int. J. Electrochem. Sci., 15 **(2020)** 2874 – 2882, doi: 10.20964/2020.04.33

International Journal of
ELECTROCHEMICAL
SCIENCE
www.electrochemsci.org

N-doped MnO_2 Nanospheres as Cathode Materials for Long Cycle Performance Lithium-Sulfur Batteries

Pengfei Huang[1,*], *Pengchao Zhang*[2], *Bo Dang*[3]

[1] School of Mechanical Engineering, Xijing University, Xi'an, Shaanxi, 710123, China.
[2] The Key Laboratory of Industrial Automaation of Shaanxi Province, Shaanxi University of Technology, Hanzhong, Shaanxi, 723001, China.
[3] Intelligent Manufacturing Research and Development Center, Xijing University, Xi'an, Shaanxi, 710123, China.
[*]E-mail: drpengfeihuang@sina.com

Received: 3 January 2020 / *Accepted:* 4 February 2020 / *Published:* 10 March 2020

N-doped MnO_2 nanospheres (NMON) are prepared and developed as the cathode materials for the lithium-sulfur batteries. First, the pristine MnO_2 nanospheres are synthesized via hydrothermal reaction method. After that, N-doping process is achieved by heating pristine MnO_2 nanospheres (PMON) under N_2 atmosphere. Finally, NMON/S composites are prepared as cathode materials. To investigate the electrochemical performance, coin batteries are assembled and tested by using the NMON/S composites as cathode materials. The electrochemical results indicate that the initial specific capacity is as high as 1118 mAh g^{-1} at 0.2 C for the NMON/S composites. The capacity of NMON/S composites remains at 810 mAh g^{-1} at 1 C after 500 cycles.

Keywords: Lithium-sulfur batteries, NMON/S composites, N-doped, Electrochemical performance, Cycle stability

1. INTRODUCTION

With the rapid development of the science and technology, an increasing number of electronic devices and electric vehicles are becoming a part of our daily life [1]. The above new electric equipment can work only being powered by energy storage systems. Besides, the traditional fuel, such as goal, gas, has become less and less [2-5]. Therefore, it is urgent for the researchers to develop new energy storage systems [6]. Furthermore, the new energy storage systems produce no pollution on the environment [7, 8]. During the past decades, many energy storage systems have been employed in many areas, including lithium-ion batteries, lithium-sulfur batteries, lithium-metal batteries [9-12]. They are used in electric vehicles, unmanned aerial vehicle and large storage equipment. In particular,

the lithium-sulfur batteries have drawn much attention for the researchers all over the world. As we all know, lithium-sulfur batteries have many advantages, 1) High specific capacity (1675 mAh g^{-1}), which is 5 times than the traditional cathode materials. 2) Considerably superior energy density (2600 Wh Kg^{-1}). 3) No production of pollution and abundant, sulfur is friendly to the environment [13, 14]. Therefore, it is important to study the lithium-batteries about cathode materials and anode protection [15].

However, to date, the lithium-sulfur batteries have failed to achieve wide application for the electric devices [16]. This is mainly caused by the following disadvantages. First, the poor electronic conductivity of the lithium-sulfur batteries leads to low active material utilization during discharge and charge processes. Second, the discharge product is easily dissolved into electrolyte, which caused shuttle effect for the polysulfide [17]. As a result, the as-prepared lithium-sulfur batteries exhibit poor cycling performance and a low specific capacity. To adress these problems, many methods have been reported, including finding suitable host materials for the sulfur, developing new anode materials and designing functional interlayers between the cathode and separator [18]. The suitable host materials can efficiently adsorb the soluble polysulfide at the cathode side to restrain the shuttle effect of the lithium-sulfur batteries. The modified lithium anode can could avoid the formation of lithium dendrite and prevent the short circuit of the lithium-sulfur batteries [19]. The functional interlayers are beneficial for hindering the migration of polysulfide from the cathode side to the anode side. Therefore, these methods are significant for improving the electrochemical performance of the lithium-sulfur batteries.

Metal oxides have been considered as the most promising host materials for sublimed sulfur. Due to a chemical bond between the metal oxide and the polysulfide, the shuttle effect of the lithium-sulfur batteries can be greatly inhibited by using metal oxides as host materials. Recently, Chen et al used N-TiO_{2-x}/RGO/S composites as cathode materials for the lithium-sulfur batteries, which demonstrated superior electrochemical performance [20]. The work claimed that the N-TiO_{2-x}/RGO/S composites could improve the electronic conductivity and inhibit the shuttle effect of the polysulfide at the same time. As a result, the electrochemical performance is enhanced. Therefore, metal oxides are useful for the application of the lithium-sulfur batteries.

In our work, we successfully prepared N-doped MnO_2 nanospheres via hydrothermal reaction method. And the as-prepared NMON/S composites are designed as cathode materials for the lithium-sulfur batteries. Due to the presence of the N-doped MnO_2 nanospheres, the cycling stability and specific capacity were greatly enhanced for the lithium-sulfur batteries. The initial specific capacity of the NMON/S composites is as high as 1118 mAh g^{-1} at 0.2 C for the NMON/S composites. The capacity of the NMON/S composites stays at 810 mAh g^{-1} at 1 C after 500 cycles.

2. EXPERIMENTAL

2.1. Preparation of N-doped MnO_2 nanospheres and NMON/S composites

Briefly, 0.8 g of $KMnO_4$ was dissolved in 50 ml deionized water and stirred for 30 min. After

that, 1.0 ml ammonia was added into the above solution and allowed to react for 1 h. Then, the solid products were collected and washed with deionized water for several times. The solid product was transferred to a high temperature furnace at 200℃ for 20 min under N_2 atmosphere. The as-prepared N-doped MnO_2 was uniformly mixed with sulfur uniformly and heated at 155 ℃ for 12 h to prepare NMON/S composites.

2.2. Materials Characterization

The morphology of the samples was observed by using scanning electron microscopy and transmission electron microscopy (SEM, TEM). The crystal structure was tested via X-ray diffraction (XRD). The sulfur content in the NMON/S composites was determined by a TG analysis under a N_2 atmosphere.

2.3. Electrochemical Test

The electrochemical performance of the NMON/S composites was tested by using coin type 2032 batteries. The as-prepared NMON/S composites were used as the cathode. The lithium film was used as anode. The separator is clegard 2300 film. The preparation of the coin batteries was conducted in glove box filled with Ar. The discharge and charge curves were obtained by using battery tester Xinwei electrochemical instrument. Electrochemical impedance spectra were conducted with an electrochemistry workstation (CHI660E).

3. RESULTS AND DISCUSSION

Figure 1a shows the morphology of the pristine MnO_2 nanospheres. As shown in Figure 1a, the as-prepared pristine MnO_2 exhibits nanosphere structure with a diameter of 100 nm. These nanospheres are uniformly distributed in the whole SEM image. After the N-doping process, N-doped MnO_2 nanospheres are successfully prepared. Figure 1b shows the SEM image of the as-prepared N-doped MnO_2 nanospheres. From the Figure 1, it can be seen that the N-doped MnO_2 nanospheres display similar morphology compared with the pristine MnO_2 nanospheres. Figure 1c-e show the TEM images of the N-doped MnO_2 nanosphere/sulfur composites. The as-prepared NMON/S composites have nanosphere structures with diameters of 100 nm, demonstrating superior sphere structure [21]. To demonstrate the element distribution of the as-prepared NMON/S composites, the corresponding elemental mapping was conducted for the NMON/S composites. As shown in Figure 1f-i, it can be clearly observed that the elements N, Mn, O and S are uniformly dispersed in the NMON/S composites. In all, the NMON/S composites are obtained via a heating method.

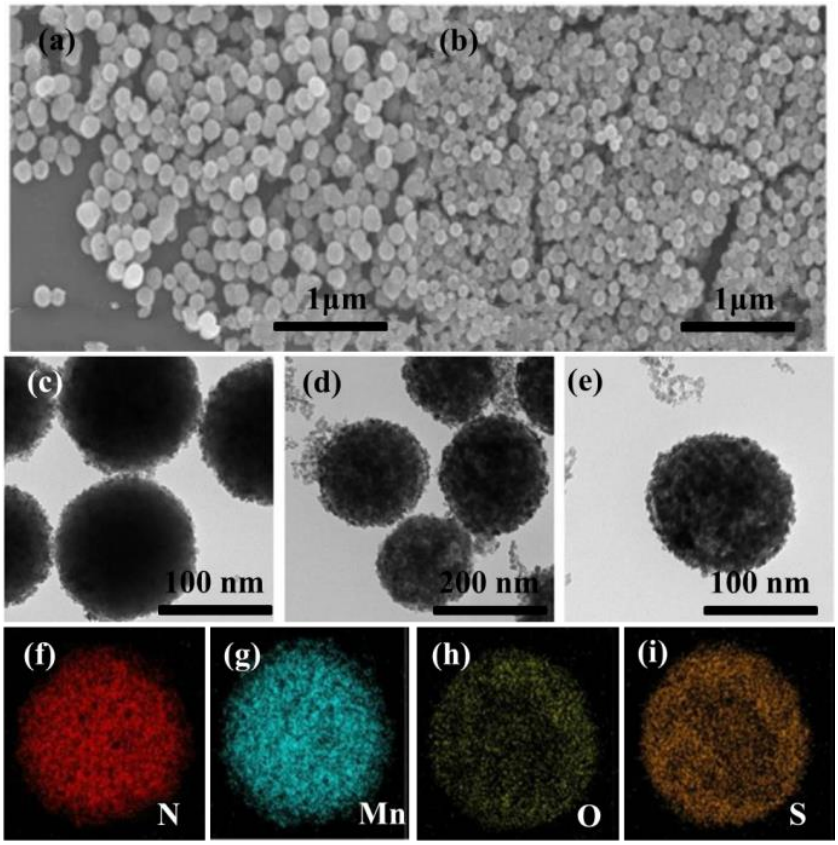

Figure 1. (a) Pristine MnO_2 nanospheres. (b) N-doped MnO_2 nanospheres. (c-e) N-doped MnO_2 nanosphere/sulfur composites. (f-i) Corresponding elemental mapping for the NMON/S composites of the elements of N, Mn, O and S.

To investigate the crystal structure of the samples, XRD patterns are displayed in Figure 2a. From the Figure 2a, the as-prepared PMON exhibits perfect crystal structure. The PMON shows typical diffraction peaks at 25°, 38°, 46° and 53°. These diffraction peaks are corresponding to crystal planes of (111), (110), (210) and (011), showing superior crystal structure [22]. After the N-doping process, the as-prepared NMON/S composites exhibit similar crystal structure as the PMON/S composites, confirming the preparation of the NMON/S composites. The as-prepared NMON/S composites shows similar diffraction peaks, which is same as the pristine sulfur. This can confirm that the element sulfur has immersed into the N-doped MnO_2 nanospheres. Sulfur content is the key to calculate the specific capacity of the lithium-sulfur batteries. To determine the sulfur content in the NMON/S composites, a TG analysis was conducted for the as-prepared NMON/S composites. As shown in Figure 2b, the NMON/S composites have weight loss between 400-550℃, which is attributed to the sulfur vapor. Therefore, the sulfur content in the NMON/S composites is about 86%.

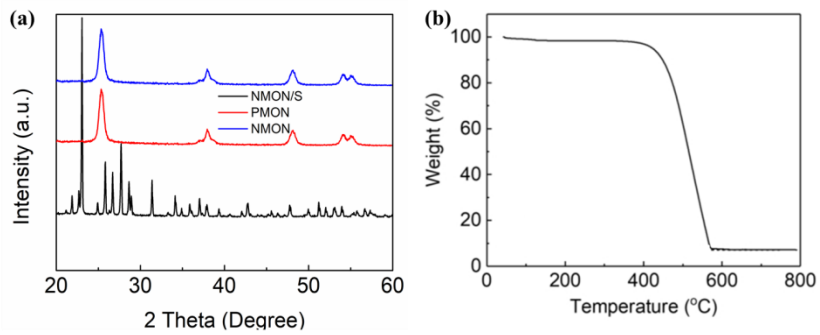

Figure 2. (a) XRD patterns of PMON and NMON and NMON/S composites. (b) TG curves of the NMON/S composites.

The superior adsorption ability for the polysulfide is important for the cathode materials in the lithium-sulfur batteries. To study the adsorption performance of the NMON and PMON materials, adsorption tests were conducted. First, polysulfide solution (Li_2S_6) was prepared by mixing pristine sulfur and solid Li_2S into the DOL/DME mixture. As shown in Figure 3a, the as-prepared mixture was stirred for 12 h. As a result, the Li_2S_6 solution was successfully synthesized. After that, the as-prepared PMON and NMON materials are added into the above Li_2S_6 solution to observe the color change with the increase of the time. As shown in Figure 3b, the as-prepared blank Li_2S_6 solution shows yellow color. For the solution dissolved NMON, it becomes colorless after 20 min, demonstrating superior adsorption ability for the Li_2S_6 [23]. However, for the PMON materials, the solution still remains yellow color. To further confirm the result, visible color change during the discharging and charging process for the PMON/S and NMON/S composite electrode were observed, respectively. As described in Figure 3c and d, after 24 h, the solution used as-prepared NMON/S electrode shows no color change. For the PMON/S electrode, it shows a yellow color after 24 h.

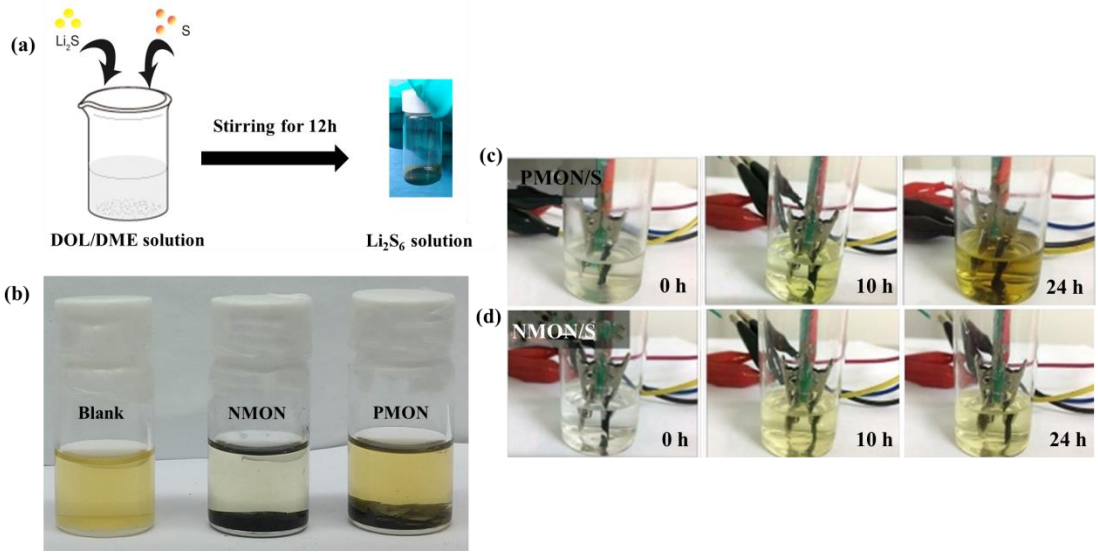

Figure 3. (a) Preparation of Li_2S_6 solution. (b) Adsorption test by using pristine MnO_2 and N-doped MnO_2. (c) and (d) Visible color change during the discharging and charging process for the PMON/S and NMON/S composite electrode, respectively.

Figure 4a and b show the constant discharge and charge curves of the NMON/S and PMON/S composite electrodes. It can be seen that the as-prepared NMON/S electrode exhibits initial high specific capacities of 1118 mAh g^{-1}, 926 mAh g^{-1}, 798 mAh g^{-1}, 625 mAh g^{-1} and 528 mAh g^{-1} at 0.2 C , 0.5 C, 1 C 2 C and 4 C, respectively. For the as-prepared PMON/S composites, the initial specific capacity is only 786 mAh g^{-1} at 0.2 C. It can be concluded that the as-prepared NMON/S electrode has much higher specific capacity than the PMON/S electrode. Besides, other information can be obtained from the discharge and charge curves. The discharge curves show two voltage plateaus at 2.3 V and 2.1 V, respectively. These platforms are related to the transformation of sulfur to high soluble polysulfide and to insoluble Li_2S_2, Li_2S. It can be concluded that the as-prepared NMON/S composites have much higher specific capacity value than the PMON/S composites [24]. This is attributed to the N-doped process, which could improve the electronic conductivity. Figure 4c shows the rate performance of the pure sulfur, NMON/S and PMON/S electrode, respectively. It can be clearly observed that the as-prepared NMON/S electrode demonstrates excellent rate capability. However, for the pure sulfur and PMON/S electrode, it shows rapid capacity fade with the increase of the current densities. This is attributed to the presence of the N-doped MnO_2 nanospheres, which could improve the electronic conductivity. This is consistent with the results obtained from the discharge and charge curves [25]. Therefore, the as-prepared NMON/S composites could endure high current densities. To confirm the superior conductivity of the as-prepared NMON/S electrode, electrochemical impedance spectrum was displayed in Figure 4d. The EIS is made up of semicircle in the high frequency and line in the low frequency. The semicircle and line represent charge and lithium-ion transport resistance, respectively. Clearly, the as-prepared NMON/S electrode shows smaller charge resistance than those of the other electrodes.

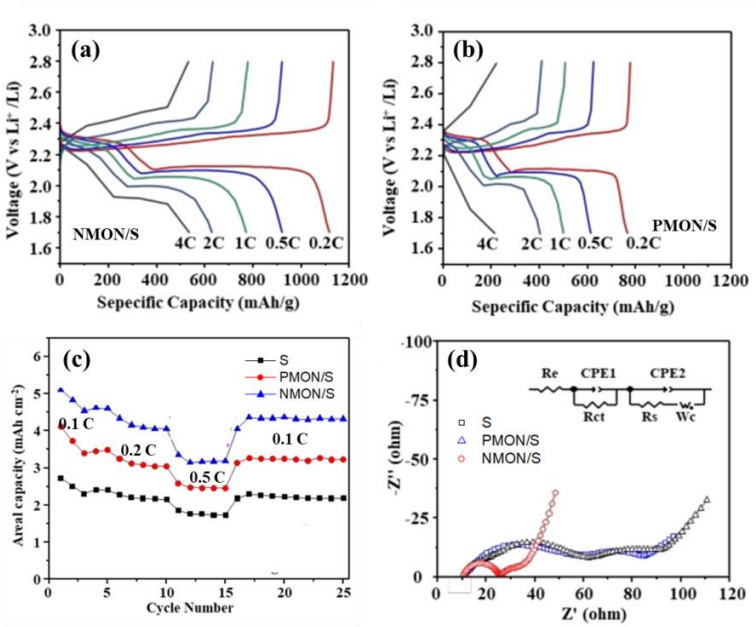

Figure 4. (a) and (b) The constant discharge and charge curves of the NMON/S and PMON/S composite electrode at different current densities, respectively. (c) Rate capabilities of the pure sulfur, PMON/S and NMON/S electrode. (d) Electrochemical impedance spectra of the pure sulfur, PMON/S and NMON/S electrode.

Figure 5a shows the long cycling performance of the electrodes. It can be seen that capacity of the as-prepared NMON/S electrode remains at 810 mAh g^{-1} at 1 C after 500 cycles. However, for the pure sulfur and PMON/S electrodes, it suffers from severe capacity fading during the electrochemical cycles. From this, the superior electrochemical performance of the NMON/S electrode is furthermore confirmed. This confirms that the as-prepared NMON/S composites are beneficial for inhibiting the shuttle effect of the soluble polysulfide [26]. Finally, the morphology of the lithium anode was observed by using scanning electron microscopy. As shown in Figure 5b and c, for the NMON/S electrode, the SEM image of the lithium anode still remains its perfect morphology. As for the PMON/S electrode, the faced lithium anode shows severe pulverization deformation, which is caused by the shuttle effect of the soluble polysulfide. In all, this further indicates that the employment of NMON/S electrode is useful for inhibiting the shuttle effect of the polysulfide.

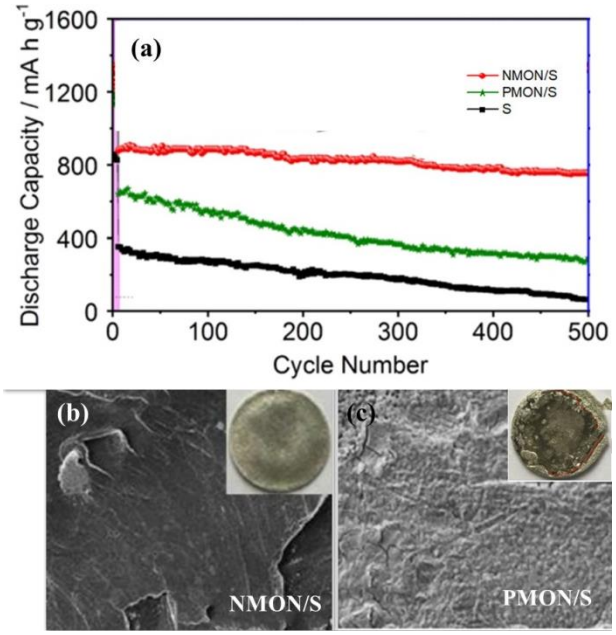

Figure 5. (a) Long cycle performance of the pure sulfur, PMON/S and NMON/S electrode at 1 C for 500 cycles. (b) and (c) SEM images of the lithium anode for the NMON/S cathode and PMON/S cathode after cycles, respectively.

To further demonstrate the superior electrochemical performance of the NMON/S composites, a table was made to compare the electrochemical performance of the cathode materials in the lithium-sulfur batteries. A listed in Table 1, the as-prepared NMON/S composites shows specific capacity of 810 mAh g^{-1} after 500 cycles at the high current density of 1 C, showing superior cycle stability at high current density. For the reported work in the literatures, it can be seen that the similar cathode materials show bad cycle stability. The capacity fades rapidly with the increase of the cycle numbers. Therefore, it can be concluded that the as-prepared NMON/S composites show excellent electrochemical performance at high current density. It is impossible for the application of the cathode materials in the lithium-sulfur batteries.

Table 1. Comparison of the electrochemical performance of the NMON/S composites with other cathode materials in the lithium-sulfur batteries.

Electrodes	Current Density	Cycle Stability	Ref
S/CPAN-800	0.1 C	862 mAh g^{-1} (100 cycles)	27
CDC/S	0.5 C	621 mAh g^{-1} (300 cycles)	28
GCN/S	0.5 c	578 mAh g^{-1} (500 cycles)	29
NMON/S	1 C	810 mAh g^{-1} (500 cycles)	This Work

4. CONCLUSIONS

In summary, to improve the cycling stability of the lithium-sulfur batteries, N-doped MnO_2 nanospheres were successfully prepared and designed as cathode materials for the lithium-sulfur batteries. As a result, the electrochemical performances of NMON/S composites were greatly improved due to the presence of the N-doped MnO_2 nanospheres. The superior electrochemical performance could be ascribed to the following tips: a) the metal MnO_2 could supply chemical adsorption for the soluble polysulfide to inhibit the migration of discharge products. b) N-doped MnO_2 is beneficial for the improvement of the electronic conductivity. In all, the issues that limit the applications of lithium-sulfur batteries are solved via using NMON/S composites. Therefore, our work may provide a promising method for developing cathode materials for use in the lithium-sulfur batteries.

ACKNOWLEDGEMENT
We thank the Shaanxi Natural Science Basic Research Project (2019JQ-923).

References

1. K. Wang, W. Y. Li, W. K. Ye, W. H. Yin, W. W. Chai, Y. Qu, Y. C. Rui and B. H. Tang, *J. Alloy. Compd*., 793 (2019) 16.
2. H. Chen, W. D. Dong, F. J. Xia, Y. J. Zhang, M. Yan, J. P. Song, W. Zou, Y. Liu, Z. Y. Hu, J. Liu, Y. Li, H. E. Wang, L. H. Chen and B. L. Su, *Chem. Eng. J*., 381 (2020) 122746.
3. X. D. Li, W. D. Zhang, B. Chen, G. X. Wu, J. X. Cai, H. Q. Wu and C. H. Jiang, *J. Solid State Chem*., 270 (2019) 304.
4. R. Dang, X. R. Ma, J. Y. Liu, M. Chen, Y. X. Zhang and J. Luo, *Int. J. Hydrogen Energ*., 43 (2018) 18754.
5. Y. Li, B. Shi, W. Liu, R. Guo, H. J. Pei, D. X. Ye, J. Y. Xie and J. L. Kong, E*lectrochim. Acta*, 260 (2018) 912.
6. J. Liu, C. W. Wang, B. Liu, X. Ke, L. Y. Liu, Z. C. Shi, H. Y. Zhang and Z. P. Guo, *Mater. Lett*., 195 (2017) 236.
7. Y. Q. Lai, P. Wang, F. R. Qin, M. Xu, J. Li, K. Zhang and Z. A. Zhang, *Energy Storage Materials*, 9 (2017) 179.
8. M. F. Chen, Q. Lu, S. X. Jiang, C. Huang, X. Y. Wang, B. Wu, K. X. Xiang and Y. T. Wu, *Chem. Eng. J*., 335 (2018) 831.
9. W. Sun, X. G. Ou, X. Y. Yue, Y. X. Yang, Z. H. Wang, D. Rooney and K. N. Sun, *Electrochim.*

Acta, 207 (2016) 198.
10. Q. N. Zhao, J. Wen, K. Q. Zhao, G. P. Ji, R. H. Wang, X. Liang, N. Hu, L. Lu, J. Molenda, J. H. Qiu and C. H. Xu, *Electrochim. Acta*, 305 (2019) 247.
11. X. K. Huang, K. Y. Shi, J. Yang, G. Mao and J. H. Chen, J. Power Sources, 356 (2017) 72.
12. B. L. Ling, A. Chen, W. F. Liu, K. Y. Liu, H. Hu and J. W. Zhang, *Mater. Lett*., 218 (2018) 321.
13. S. Y. Tan, Z. L. Yang, H. Y. Yuan, J. Zhang, Y. H. Ynag and H. T. Liu, *J. Alloy Compd*., 791 (2019) 483.
14. G. P. Chen, X. Song, S. Q. Wang, X. Z. Chen and H. H. Wang, *J. Power Sources*, 408 (2018) 58.
15. M. Q. Liu, Q. H. Zhao, H. Liu, J. L. Yang, X. Chen, L. Y. Yang, Y. H. Cui, W. Y. Huang, W. G. Zhao, A. Song, Y. T. Wang, S. X. Ding, Y. L. Song, G. Y. Qian, H. B. Chen and F. Pan, *Nano Energ*., 64 (2019) 103942.
16. S. N. Yang, Y. Cheng, X. Xiao and H. Pang, *Chem. Eng. J*., 384 (2020) 123294.
17. Z. F. Ma and T. B. Zhao, *Electrochim. Acta*, 201 (2016) 165.
18. J. J. Shi, S. L. Wang, Q. Wang, X. Chen, X. Y. Du, M. Wang, Y. J. Zhao, C. Dong, L. M. Ruan and W. Zeng, *J. Power Sources*, 446 (2020) 227345.
19. Y. J. Huang, Y. L. Lin and W. S. Li, *Electrochim. Acta*, 99 (2013) 161.
20. G. F. Chen, J. H. Li, N. Liu, Y. Zhao, J. G. Tao, Z. Bakenov and Y. G. Zhang, Electrochim. Acta, 326 (2019) 134968.
21. A. M. Hashem, H. Abuzeid, M. Kaus, S. Indris, H. Ehrenberg, A. Mauger and C. M. Julien, *Electrochim. Acta*, 262 (2018) 74.
22. Z. L. Xu, J. K. Kim and K. Kang, *Nano Today*, 19 (2018) 84.
23. Y. J. Zhong, X. M. Xu, Y. Liu, W. Wang and Z. P. Shao, *Polyhedron*, 155 (2018) 464.
24. J. Zhou, N. Liu, W. L. Cai, C. Guo, K. L. Zhang, J. B. Zhou, Y. C. Zhu and Y. T. Qian, *Electrochim. Acta*, 218 (2016) 243.
25. F. Nitze, K. Fossum, S. Z. Xiong, A. Matic and A. E. Palmqvist, *J. Power Sources,* 317 (2016) 112.
26. S. C. Jung and Y. K. Han, *J. Power Sources*, 325 (2016) 495.
27. Y. Liu, X. H. Zhao, G. S. Chauhan and J. H. Ahn, *Appl. Surf. Sci*., 380 (2016) 151.
28. Y. J. Wei, Y. Q. Tao, C. F. Zhang, J. T. Wang, W. M. Qiao, L. C. Ling and D. H. Long, *Electrochim. Acta,* 188 (2016) 385.
29. Z. Meng, Y. Xie, T. W. Cai, Z. X. Sun, K. M. Jiang and W. Q. Han, *Electrochim. Acta*, 210 (2016) 829.